

# Efficient Interleaving Schemes of Volume Holographic Memory

Seunghoon Han, Minseung Kim, Byungchoon Yang, and Byoungho Lee\*

*School of Electrical Engineering, Seoul National University,  
Seoul 151-744, KOREA*

(Received November 14, 2002)

Like the conventional digital storage systems, volume holographic memory can be deteriorated by burst errors due to its high-density storage characteristics. These burst errors are caused by optical defects such as scratches, dust particles, etc. and are two-dimensional in a data page. To deal with these errors, we introduce some concepts for describing them and propose efficient two-dimensional interleaving schemes. The schemes are two-dimensional lattices of an error-correction code word and have equilateral triangular and square structures. Using these structures, we can minimize the number of code words that are interleaved and improve the efficiency of the system. For large size burst errors, the efficient interleaving structure is an equilateral triangular lattice. However, for some small size burst errors, it is reduced to a square lattice.

*OCIS codes* : 090.7330, 090.4220.

## I. INTRODUCTION

A burst noise is a common problem in many of the digital communication media. This noise produces a burst error, a cluster of consecutive errors of symbols. The symbol is an error-correction unit of an error-correction code (ECC) and is composed of one to several bits according to the ECC structure. Each ECC word is composed of several number of these symbols [1]. In volume holographic memory (VHM), the burst error becomes very troublesome because digital data are stored and processed with high density. In general, interleaving is a way of solving burst errors by permuting symbols of several ECC words. The interleaving for VHM has to consider its two-dimensional characteristics, which originate from the fact that data are processed using a two-dimensional array of bits, i.e., a data page. In a data page, a burst error also occurs over some two dimensional area in general. Several interleaving techniques to deal with this problem have been proposed.

These techniques are categorized as inter-page parallel one-dimensional interleaving and intra-page two-dimensional interleaving. The inter-page parallel one-dimensional interleaving is used for inter-page burst errors to deal with burst noises which occur over several data pages [2,3]. It views each bit in a data page as one communication channel and many data streams (i.e., streams of ECCs) are processed in parallel using

a collection of these channels, the data page. Therefore, each code word has a certain fixed location in a data page and its symbols are spread and interleaved over several data pages. On the contrary, for burst errors within a data page, we can make use of intra-page two-dimensional interleaving. Let it be called two-dimensional interleaving in the following. Given the number of ECCs and the size of an interleaving area, this interleaving technique spreads symbols of each code word in a two-dimensional grid plane. Almeida *et al.* [4] made two-dimensional interleaving which maximizes the minimum Euclidean distance between the spread code word symbols by introducing the set-partitioning concept. Blaum *et al.* [5] proposed minimizing the number of interleaved code words in multi-dimensional interleaving, and hence improving the interleaving efficiency. By reducing the number of code words interleaved (i.e., interleaving degree), the code word length can be increased so that overall error performance is improved. They considered two-dimensional interleaving minimizing the interleaving degree to overcome two-dimensional  $t$  consecutive ( $t$ -interleaved) errors. What we propose in this paper is a scheme of an efficient two-dimensional interleaving according to the burst error characteristic in the data page. The characteristic we consider here is that there exists a maximum diameter for the burst errors to deal with. Blaum *et al.* minimized the interleaving degree considering the two-dimensional size of the burst error ( $t$ -interleaved) [5]. In this paper, we focus on minimiz-

ing the number of the interleaved code words for the maximum diameter of burst errors. Here, we measure the diameter of the burst error and other distances using the Euclidean metric ( $d_2(x_1, y_1; x_2, y_2) = [(x_1 - y_1)^2 + (x_2 - y_2)^2]^{1/2}$ ,  $x_1, y_1, x_2, y_2 \in R$ ). This is meaningful when burst errors in the data page have random shapes so that the two-dimensional sizes are not fixed, but have a certain limit on their diameters with random orientation. If we apply the two-dimensional interleaving of Blaum *et al.*'s for this case, we can see that there occur some redundant code words (additional interleaving degree) since the method uses the metric  $d_1(x_1, y_1; x_2, y_2) = |x_1 - y_1| + |x_2 - y_2|$  to measure inter-symbol distance of each code word. We note that radial spreading structure of two-dimensional interleaving was proposed when the optical system has some misalignment with the threshold detection [6]. For the simplification of the problem, we excluded the position dependence of the random error rate due to the misalignment.

We consider VHM as a channel of random burst erasure process, where two-dimensional burst errors occur at random positions, with random shapes in a data page. Here, it is assumed that for a given VHM system, the mechanism of burst errors can be understood and exploited to determine the maximum diameter of burst errors [1]. Then we introduce some parameters to describe these burst errors, and using these parameters we propose efficient two-dimensional interleaving schemes of lattice structure. These interleaving schemes minimize and equalize the Euclidean distances between neighboring lattice points (i.e., symbols of one code word) so that the number of interleaved code words is minimized when the maximum diameter of burst error is given.

## II. TWO-DIMENSIONAL BURST ERROR

### 1. Two-dimensional burst noise

Generally, the  $4f$  optical system is used in the VHM. (Fig. 1) A data page is displayed on a spatial light modulator (SLM) at the input plane of the  $4f$  system. The information of the data page is carried by an object beam from a laser source and recorded in the holographic material by use of interference with a reference beam from the same laser. The recording material is located at the Fourier plane of a lens (Fourier hologram) or some distance off the Fourier plane (Fresnel hologram) [7]. When retrieving the data, the same reference beam used in the recording procedure illuminates the holographic material and the regenerated data page information is imaged onto the CCD at the

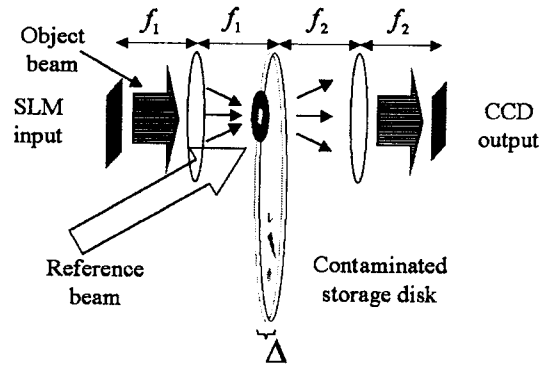


FIG. 1. The  $4f$  optical system of VHM. Storage material has some thickness and there exists a boundary between the material and air, which is out of the Fourier plane.

output plane of the  $4f$  system.

Because the VHM uses three-dimensional gratings with sufficiently large sizes (much larger than the laser beam's wavelength  $\lambda$ ) to increase its storage density, the holographic storage material should have some three-dimensional volume. Especially, along the longitudinal direction of the  $4f$  system, a thickness ( $\Delta$ ) of several millimeters is required for the storage material [8]. As a result, for both the Fourier hologram and the Fresnel hologram, there exist boundary planes, which are out of the Fourier plane. The boundary planes might be contaminated by dusts or defects.

Fig. 2 shows CCD-detected image with some burst noises at the output plane of the  $4f$  system. These

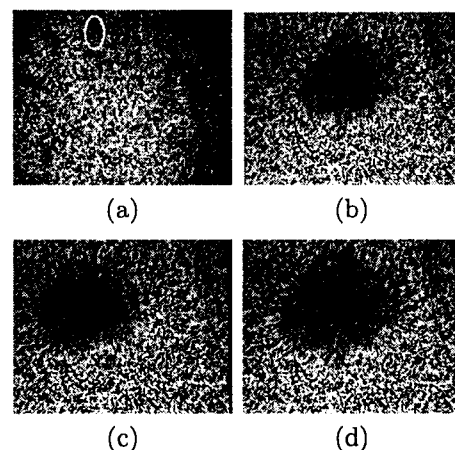
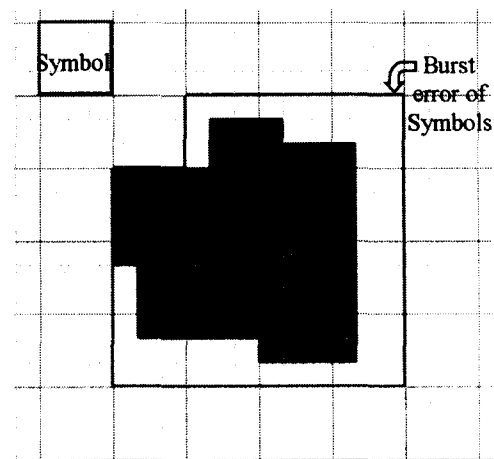


FIG. 2. Burst noise characteristics. (a) Burst noises due to some dust particles at the off-Fourier plane (the white-circled area, for example). (b) Burst noise caused by a contamination source (inky spot) at the off-Fourier plane (c) Burst noise translation when the contamination source translated horizontally. (d) Burst noise enlargement when the contamination source moved toward the Fourier plane.

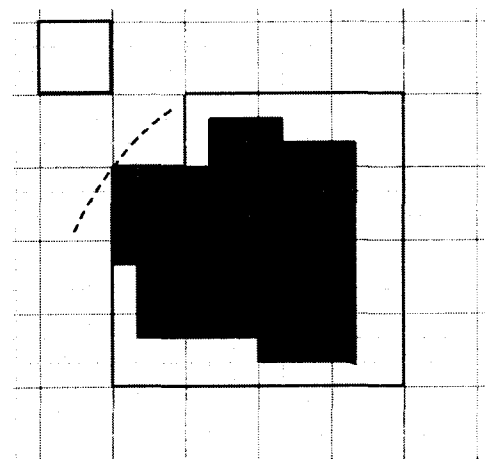
burst noises are caused by some contamination a few millimeters behind the Fourier plane. The numerical aperture of SLM used in the experiment is about 0.1. In Fig. 2 (a), the contamination source is several minute dust particles. Here, we can see that the overall image is somewhat blurred and find several two-dimensional burst noise areas where noise occurs in (1,0) intensity data. To examine relationships further between the contamination source and burst noise, we pointed a small inky spot (diameter 0.5 mm) on a slide glass a few millimeters (5 mm) behind the Fourier plane. Then the burst noise occurred quite apparently as in Fig. 2 (b). When the inky spot was translated horizontally in the transverse plane, there occurred corresponding burst noise translation (Fig. 2 (c)). And when the inky spot was moved closer to the Fourier plane in the longitudinal direction, the burst noise was enlarged (Fig. 2 (d)). In both cases, we note that the shape of the burst noise was not changed. It is easy to interpret these results using the ray optical tracing of each data bit. Each ray from the data bit propagates in the optical system and when it meets a contamination source, its propagation is disturbed. Therefore, we can conclude that the shape, size, and location of the contamination source determine the ray bundle of the noise data bits and the burst noise characteristics in the output plane. There are other sources of burst noise in VHM like clusters of dead pixels of SLM or CCD. In these cases, it is also possible to understand the mechanism and statistics of burst noises. As a result, it is appropriate to assume that if a VHM system is designed, we can find burst noise characteristics of the system and exploit them to construct a suitable interleaving structure.

## 2. Two-dimensional burst error and symbolic radius

In the above, we saw that burst noise makes it difficult to decide 1's and 0's in the retrieving process. To handle this noise more strictly, we introduce the concept of burst erasure. An erasure is a state of a transmitted binary data in a digital communication channel that cannot be distinguished as either 1's or 0's. Using this concept in our VHM case, we denote the damaged bit of which the information is estimated to be corrupted as an erased bit. When the retrieved image of VHM has a burst noise, there are also some erased bits in the burst noise, whichever detection method is used. For example, if the threshold detection scheme is applied to the retrieving process, these erased bits may have intensities in the range of the overlapped area of distribution functions of 1's and 0's [9]. Similarly, when the modulation code is used in the detection, bits for which intensity information



(a)



(b)

FIG. 3. (a) Burst erasure (cluster of erased bits) causes burst error of symbols embracing it. Each symbol is composed of  $3 \times 3$  bits. (b) A burst erasure is characterized by the longest length across it in unit of symbols (symbolic radius, bold arrow).

is changed can be the erased bits [10]. We call the cluster of these erased bits a burst erasure. (Fig. 3)

In Fig. 3, several symbols of ECC are tiled in a matrix form. Each symbol is composed of  $3 \times 3$  bits in this example. In ECC, a symbol is a unit of error correction and generally is composed of one to several bits. Even one bit error might produce error of the symbol that contains the error bit. Therefore, in Fig. 3, we can distinguish a cluster of symbol errors containing the burst erasure area. This is the two-dimensional burst error of symbols.

We can find some relations between burst erasure and burst error. To deal with these relations, we introduce a parameter for the burst erasure. It is possible to draw a line with the longest length across the

burst erasure. Then we can get the numerical value of the length of this line in a symbol unit. We call this length the *symbolic radius*  $R$ . In Fig. 3 (b), the symbolic radius is about 4.3 symbols in Euclidean metric (i.e.  $\sqrt{3.3^2 + 2.7^2}$ ). Here we can have an assumption that for a given system and given contamination source characteristics, there exists a maximum symbolic radius of burst erasures. In the following, we make interleaving strategies for the burst error problem using this maximum symbolic radius.

### III. INTERLEAVING SCHEMES

#### 1. Extended circle of burst erasure

In the conventional one-dimensional interleaving, an important parameter is the maximum burst error length of a system, i.e.,  $B$  symbols. In this case,  $B$  code words are rearranged so that symbols of each error-correction code word are spaced by  $B$  symbol intervals. By doing this, we can change the  $B$  consecutive symbol errors (i.e., burst error) into one symbol error for each of the interleaved  $B$  code words. Because each of these  $B$  code words has only one damaged symbol by a burst erasure of length  $B$ , the burst error problem is transformed into one symbol error problem for each code word. As a result,  $B$  symbols from each code word form the unit of permutation [1,6]. However, in the two-dimensional case, it is required to consider the size, shape, and ordering of the permutation units in relation with the burst error size, i.e. symbolic radius. To deal with these permutation units in the two-dimensional domain, we make use of some terminologies in the solid-state crystal lattice.

Fig. 4 shows relations between the area of possible burst erasure and the symbolic radius by taking one symbol as an origin (numbered '1' in Fig. 4). By translating and drawing a circle with a line of symbolic radius in contact with the origin symbol, we can draw an extended circle of possible burst erasure. If there is any other symbol from the same code word of the origin symbol within or at the boundary of the extended circle, then it becomes possible that more than one symbol in the code word are corrupted by a burst erasure. In this case, there is no advantage of the interleaving. Therefore, in order to obtain an effective interleaving, the origin symbol of the extended circle must be surrounded by symbols from other code words within the boundary of the extended circle. As a result, the extended circle and its boundary need to be filled with symbols from different code words (different numbers in Fig. 4). Other symbols of the code word that contains the origin symbol must be located out of the extended circle so that there is no overlapping with the extended circle. For all the symbols

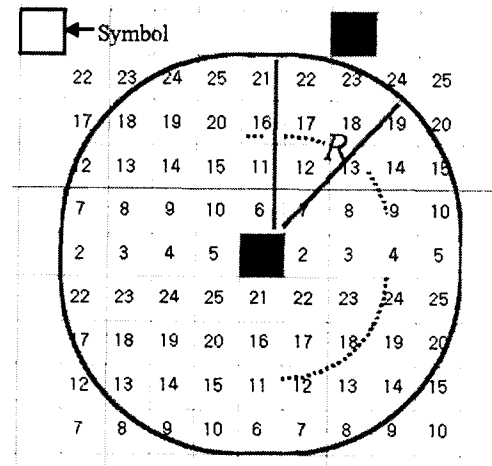


FIG. 4. Extended circle of burst erasures when symbolic radius is 4. The extended circle and its vicinities mean the area of possible burst erasure. The origin symbol (numbered '1') is surrounded by symbols from other code words within the boundary of the circle (numbered '2'–'25').

in a data page, we can repeat this procedure two-dimensionally. For each of them, we can draw an extended circle and fill the inner area by symbols from different code words and then position other symbols of the same code word out of the circle. Hence the symbol positioning has a periodicity in the two-dimensional domain and it will become a two-dimensional lattice structure with some lattice constants and primitive unit cells [11]. In the following, we will deal with the characteristics of these two-dimensional lattices in relation with the maximum symbolic radius.

#### 2. Equilateral triangular lattice

Generally, an ECC is characterized by  $(n, k, t)$ , where  $n$  is the code word length measured by symbols,  $k$  is the message symbol length, and  $t$  is the error correction capability. The error correction capability is increased with the increase of the redundancy  $n - k$ . However, although we can improve the error correction capability by introducing more redundancy, this introduces a problem in that the storage efficiency becomes worse. As  $n - k$  is increased, the ratio of the original message  $k$  over the whole code word (i.e. code rate  $k/n$ ) is reduced. Therefore, there exists a tradeoff between the error correction capability and the storage efficiency (code rate).

When the required error correction capability  $t$  is fixed in relation with  $n - k$ , the code rate  $k/n$  can be increased by increasing the code word length  $n$ . And if the code rate is fixed, by increasing the code word

length  $n$ , we can improve the error correction capability of the ECC and the reliability of the system. In both cases, we can have an improvement of the system performance with the increase of the code word length. For the case of the two-dimensional interleaving in VHM, we can increase the code word length by reducing the number of code words being interleaved within a given interleaving area. The relation is

$$N_x \times N_y = Sn, \tag{1}$$

where a rectangular array of  $N_x \times N_y$  symbols is the interleaving area. It is composed of  $S$  interleaved code words of which the length is  $n$  symbols. We can see that as the number of the interleaved code words  $S$  is reduced, the inter-symbol distances of each code word become shortened and the code word length can be increased.

Considering the burst error problems, there arises one condition that must be satisfied. As we have found in the above, the condition is that symbols of each code word should be positioned so that any two of them will not be covered simultaneously by one extended circle of the maximum symbolic radius of the burst erasures. As in Fig. 5 (a), we can position three symbols of a code word most closely in an equilateral triangular form satisfying this requirement. At first, by taking an origin with a given symbol  $A$ , draw an extended circle and position symbol  $B$  in the outside of the circle. Then using symbol  $B$  as an origin, draw another extended circle and locate the third symbol  $C$  outside of both circles. As a result, we obtain a triangular lattice structure of symbols. In this lattice structure, there exist three lattice constants,  $AB, BC, CA$ . When the relative positions of these three symbols are chosen so that the lattice constants are equalized with smallest lengths, the interleaving becomes most efficient, i.e., the least number of code words are interleaved as the following.

Fig. 5(b) shows a construction of the equilateral triangular lattice structure, i.e., the extension of Fig. 5(a) over the two-dimensional structure. For each symbol of a code word, we can repeat the above spreading procedure. Here, symbols of certain code word indicated as shaded square are dispersed. We note that there can exist only three lattice constants. Borrowing the concept of crystal lattice in solid-state physics, we can define a two-dimensional primitive unit cell, which is the smallest unit area that can construct the whole structure by translating it without any overlapping. Note that the primitive unit cell is not triangular and it is not unique. In Fig. 5(b), we can find with ease that the primitive unit cell can be a diamond of  $ABCD$ . Also, we can find another primitive unit cell with different shape of a rectangular array  $AD'$ . The area of this primitive unit cell becomes the number of the interleaved code words  $S$ .

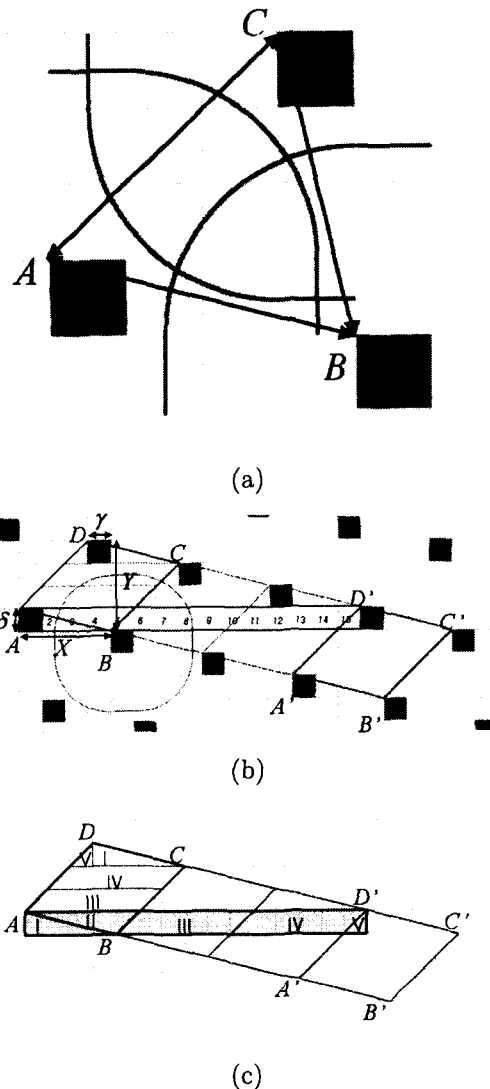


FIG. 5. Construction of the equilateral triangular lattice interleaving (a) Equilateral triangular structure provides the most efficient interleaving lattice. (b) The primitive unit cells of the lattice. (c) The relationship between primitive cells of different shape.

The infimum (the greatest lower bound) of  $S$  is

$$S_{inf} = \frac{\sqrt{3}}{2}(R + 1)^2 \tag{2}$$

when all the lattice constants are equalized and minimized to the length  $R + 1$  as an ideal case. Here, 1 is due to the length of a symbol itself. The infimum of this case is obtained as an area of the diamond composed of two equilateral triangles.

When the  $y$ -directional transition  $Y$  between  $B$  and  $D$  is a multiple of the  $y$ -directional transition between  $A$  and  $B$  like

$$Y = \alpha\delta, \quad (3)$$

where  $\alpha$  and  $\delta$  are integers,  $ABCD$  can be reorganized as  $AD'$  with some division and translations [11]. Fig. 5(c) shows the reorganizing diamond primitive unit cell into the rectangular unit cell. There exists correspondence between the regions I, II, III, IV, V of the diamond  $ABCD$  and those of the rectangle  $AD'$ . The rectangle  $AD'$  can be obtained from the diamond  $ABCD$  with  $\overrightarrow{DA}$  translation of region I, region II itself, the  $\overrightarrow{AB}$  translation of region III, the  $\overrightarrow{CD}$  translation of region IV, and the  $\overrightarrow{DD'}$  translation of region V. Here, the definition of  $\overrightarrow{XY}$  transition of region I is parallel movement of region I with length  $|\overrightarrow{XY}|$  and direction  $\overrightarrow{XY}/|\overrightarrow{XY}|$ . This rectangle ( $AD'$ ) of symbols also constitutes the whole lattice structure with repeated translations. It is another version of the primitive unit cell. We can know that these primitive unit cells have size  $S$  of 15 symbols.

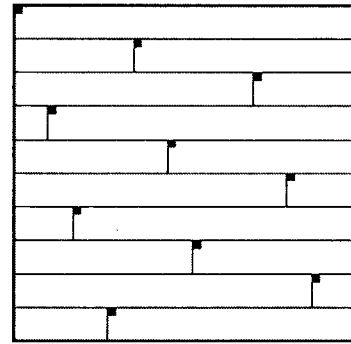
Now we can conclude a scheme of an efficient two-dimensional interleaving. When the system characteristic of the maximum symbolic radius  $R$  is determined, it is possible to construct the equilateral triangular lattice structure. Then with some division and translations, the rectangular primitive unit cell and its size  $S$  are acquired. We can allocate different code words to different positions in this unit cell and then symbols of each code word are always located at their own positions over all the primitive unit cells. As a result, symbols of  $S$  code words are interleaved two-dimensionally in a data page with an efficient equilateral triangular lattice structure.

From Fig. 5(b), the properties of the primitive unit cell are explained using the  $x$ -directional transition  $X$ ,  $y$ -directional transition  $\delta$  between  $A$  and  $B$ , and the  $x$ -directional transition  $\gamma$ ,  $y$ -directional transition  $Y$  between  $B$  and  $D$ . The size  $S$  of a primitive unit cell is derived from the rectangular primitive unit cell  $AD'$  and Eq. (3) as

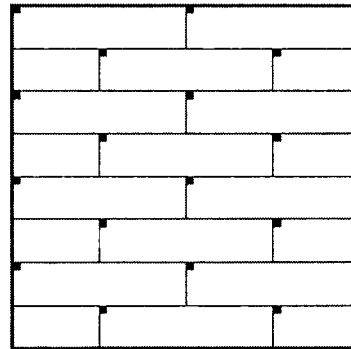
$$S = (\alpha X - \gamma)\delta = XY - \gamma\delta \quad (4)$$

We can see that  $\delta$  symbols in the  $y$ -direction are lined  $x$ -directionally by  $\alpha X - \gamma$  times.

For the last, the size of the data page or an interleaving area is determined as follows. The  $x$ -directional length  $N_x$  of an interleaving area measured by symbols must be chosen as integer multiples of  $x$ -directional width  $\alpha X - \gamma$  of the rectangular primitive cell ( $AD'$ ). Likewise the  $y$ -directional length  $N_y$  should be some integer multiples of  $y$ -directional height  $\delta$  of the rectangular primitive cell (Fig. 6). When the rectangular primitive unit cell is positioned at the boundary of the interleaving area, the outer part of the unit cell should be cut and translated to the opposite region of the interleaving area using modulo  $N_x$  operation.



(a)



(b)

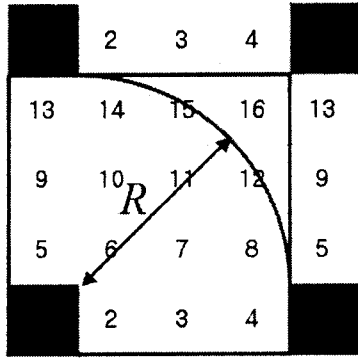
FIG. 6. The relation of an interleaving area and rectangular primitive unit cells (a) One primitive unit cell lies in horizontal direction. (b) Two primitive unit cells lie in horizontal direction.

Fig. 6(a) shows a case when only one rectangular primitive unit cell lies in  $x$ -direction and Fig. 6(b) shows another case when two unit cells lie in  $x$ -direction. More multiple rectangular unit cells can also lie along the  $x$ -direction.

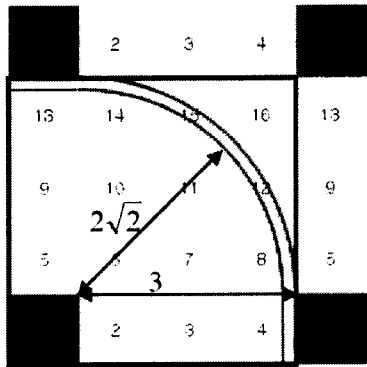
### 3. Square lattice

There exist certain ranges of the maximum symbolic radius  $R$ , where the above equilateral triangular lattice is not the most efficient interleaving structure. In Fig. 7(a), we can see that the extended circle of burst erasure and its boundary region form a square of the possible burst error. It happens when the possible burst erasure covers the origin symbol and the outermost corner symbol of the square simultaneously. The ranges of a symbolic radius for this case are determined as  $(\sqrt{2}, 2)$  and  $(2\sqrt{2}, 3)$  using geometrical calculations. For example, Fig. 7(b) shows one possible case corresponding to  $(2\sqrt{2}, 3)$ . In this case, the  $4 \times 4$  square symbol array is influenced by the extended circle of burst erasure. We solved the problem assuming that the corner symbol is erased when any part of

IV. CONCLUSION



(a)



(b)

FIG. 7. Square lattice and its square primitive unit cell. (a) The square unit cell is repeated in the two-dimensional interleaving area. (b) The square lattice case for the symbolic radius of  $(2\sqrt{2}, 3)$ .

it is covered by the symbolic radius. And in these ranges, the most efficient lattices are square lattices with lattice constant  $L$  given by

$$L = [R] + 1, \tag{5}$$

where  $[R]$  means the smallest integer no less than  $R$ . The primitive unit cell then becomes square of  $L \times L$  symbols of which the size is

$$S = ([R] + 1)^2. \tag{6}$$

In these cases, to make an equilateral triangular lattice interleaving has no advantage in efficiency.

In VHM, due to the two-dimensional characteristics of the data page, the burst error occurs two-dimensionally by some optical defects. Unlike the one-dimensional burst errors in the conventional digital data communications, in this case, the burst error has some shapes and sizes. In order to deal with them, we have introduced the notions of burst erasure and symbolic radius. When a burst noise occurs in a data page, the cluster of distorted bits (burst erasure) has a maximum diameter across it. We call this maximum diameter the symbolic radius of burst erasure. In relation with the principal contamination source of burst error and the designed optical system of VHM, it has been assumed that we can predict or decide the maximum symbolic radius of burst erasures to overcome. Then by using this maximum symbolic radius, we constructed the two-dimensional interleaving schemes excluding the effect of burst error shapes.

When the maximum symbolic radius is given, for any symbol in a data page, we can draw an extended circle with the maximum symbolic radius as its radius taking the symbol as a center of the circle. Then any other symbols of the same code word of the centered symbol should not be located within or at the boundary of the extended circle. By repeating this procedure for all the symbols, we can position symbols of each code word two-dimensionally with some periodicities. These periodicities form the two-dimensional lattice constants of the code word symbols.

The lattice constants of the two-dimensional lattices become the inter-symbol-space of the two-dimensional interleaving and the size of the primitive unit cell becomes the number of interleaved code words. When the lattice forms an equilateral triangular lattice structure, the interleaving efficiency is highest. However, for small size burst erasures of symbolic radius  $(\sqrt{2}, 2)$ ,  $(2\sqrt{2}, 3)$ , the interleaving lattices are reduced to square lattices of lattice constants 3 and 4 in each. Here, the numerical values are calculated assuming that the corner symbol is erased by only small fraction coverage of a symbolic radius. For both cases, we can have an insight about the two-dimensional interleaving of VHM by use of the rectangular primitive unit cell and its tiling with some two-dimensional translations.

In our research, all the symbols that we used have square shapes. To make problems simpler, we have only considered symbols composed of square number of bits. However, for more practical cases, it is worthy to examine non-square shape symbols as interleaving units. In this case, we can expect some changes in the range of the maximum symbolic radius where the lattice becomes a square or even a rectangular form.

## V. ACKNOWLEDGEMENT

The authors acknowledge the support by the Ministry of Science and Technology of Korea through the National Research Laboratory Program.

\*Corresponding author : byoungcho@snu.ac.kr.

## REFERENCES

- [1] G. C. Clark and J. B. Cain, *Error-Correction Coding for Digital Communications*, (New York:Plenum Press, 1981).
- [2] M. A. Neifeld and J. D. Hayes, *Appl. Opt.* **34**, 8183 (1995).
- [3] S. Jeon, S. Han, B. Yang, K. M. Byun, and B. Lee, *Jap. J. Appl. Phys.* **40**, 1741 (2001).
- [4] C. de Almeida and R. Palazzo Jr., *Electron. Lett.* **32**, 538 (1996).
- [5] M. Blaum, J. Bruck, and A. Vardy, *IEEE Trans. Inform. Theory* **44**, 730 (1998).
- [6] W. C. Chou and M. A. Neifeld, *Appl. Opt.* **37**, 6951 (1998).
- [7] H. -Y. S. Li and D. Psaltis, *J. Opt. Soc. Amer. A.* **12**, 1902 (1995).
- [8] H. -Y. S. Li and D. Psaltis, *Appl. Opt.* **33**, 3764 (1994).
- [9] X. Yi, P. Yeh, and C. Gu, *Opt. Lett.* **19**, 1580 (1994).
- [10] G. W. Burr, J. Ashley, H. Coufal, R. K. Grygier, J. A. Hoffnagle, C. M. Jefferson, and B. Marcus, *Opt. Lett.* **22**, 639 (1997).
- [11] N. W. Ashcroft and N. D. Mermin, *Solid State Physics*, (Saunders College Publishing, 1976).